CrystEngComm

ROYAL SOCIETY OF CHEMISTRY

PAPER

View Article Online
View Journal

Cite this: DOI: 10.1039/d5ce00572h

Modulating the crystalline forms of silver–sulfadiazine complexes by mechanochemistry

Daniela R. Ferreira,†[ab] Anaïs Portet,†[h] Paula C. Alves,[abc] Patrícia Rijo,[de] Clara S. B. Gomes,[f] M. Teresa Duarte,[a] Ivan Halasz,[g] Evelina Colacino,[h] Franziska Emmerling[i] and Vânia André *[ab]

Mechanochemical synthesis of pharmaceutical compounds has gained significant attention due to its potential to overcome traditional synthetic challenges while offering the possibility of improving the physicochemical properties of drugs. This study delves into the mechanochemical synthesis of silver sulfadiazine (AgSD) coordination compounds, obtained under different mechanochemical stress and processing conditions. The aim of this work was to investigate the influence of mechanochemical conditions on the selectivity in the preparation of AgSD coordination compounds. Through a series of experiments, we demonstrate the successful synthesis of two different AgSD coordination networks, using high-energy ball milling. By strategically manipulating the starting materials and milling parameters — including milling time, milling frequency, type of mechanical stress (as determined by different milling devices), and the presence of co-milling agents — we were able to control the product outcome. As a result, we achieved two different forms of silver-sulfadiazine metal frameworks, one of which was not previously disclosed. The crystal structure of the new form, obtained from high resolution PXRD synchrotron data, was compared with the previously known structure of a silver sulfadiazine compound. The in-depth antimicrobial activity systematic study of these AgSD forms on the generic systems showed increased antibacterial activity when compared to sulfadiazine. This research sheds light on the mechanochemical synthesis of silver sulfadiazine complexes. The obtained knowledge may guide the development of novel synthetic strategies for other drug molecules, leading to improved drug performance, stability, and therapeutic outcomes.

Received 2nd June 2025,
Accepted 25th July 2025

DOI: 10.1039/d5ce00572h

rsc.li/crystengcomm

Introduction

Microbial infections significantly impair wound healing in burn patients, contributing to high mortality rates. It is estimated that over 180 000 deaths occur annually due to burns, with approximately 75% resulting from bacterial infections at the burn site.[1] Burn wound infections thus represent a major clinical challenge, requiring effective treatments that simultaneously fight the infection and promote healing. Conventional antimicrobial therapies face limitations, including rising bacterial resistance and insufficient wound healing support, emphasizing the need for new antimicrobial agents with broad-spectrum efficacy and improved delivery.

As part of our ongoing investigation on the mechanochemical preparation of metallodrugs, a special class of active pharmaceutical ingredients (APIs), we have previously reported the mechanochemical syntheses of the gastrointestinal drug bismuth subsalicylate (Pepto-Bismol®),[2] and the antibacterial agent silver sulfadiazine[3] (AgSD, Silvadene®), an essential medicine listed by the World Health Organization (WHO)[4] for burn treatment.[5,6] AgSD exhibits broad-spectrum antibacterial activity, combining the antiseptic effects of silver ions[7,8] with the antibiotic properties of sulfadiazine.[5]

Sulfonamides, including sulfadiazine (SD, Fig. 1), are a class of chemotherapeutics effective against bacterial

[a] Centro de Química Estrutural, Institute of Molecular Sciences, Chemical Engineering Department, Instituto Superior Técnico, Universidade de Lisboa, Av. Rovisco Pais, 1049-001 Lisboa, Portugal. E-mail: vaniandre@tecnico.ulisboa.pt
[b] Associação do Instituto Superior Técnico para a Investigação e Desenvolvimento (IST-ID), Avenida António José de Almeida, 12, 1000-043 Lisboa, Portugal
[c] Faculdade de Farmácia da Universidade de Lisboa, Av. Prof. Gama Pinto, 1649-003 Lisboa, Portugal
[d] Universidade Lusófona's Research Center for Biosciences and Health Technologies (CBIOS), Campo Grande 376, 1749-024 Lisboa, Portugal
[e] Research Institute for Medicines (iMed. ULisboa), Faculty of Pharmacy, Universidade de Lisboa (UL), Av. Prof. Gama Pinto, 1649-003 Lisboa, Portugal
[f] LAQV-REQUIMTE, Faculdade de Ciências e Tecnologia, Universidade NOVA de Lisboa, 2829-516 Caparica, Portugal
[g] Ruđer Bošković Institute, Bijenička c. 54, Zagreb, Croatia
[h] ICGM, Univ Montpellier, CNRS, ENSCM, 34293 Montpellier, France
[i] Federal Instutite for Materials Research and Testing, Richard-Willstätter-Str. 11, 12489 Berlin, Germany
† Equal contribution.

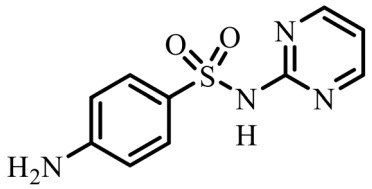

Fig. 1 Chemical structure of sulfadiazine (SD).

infections. SD is a broad-spectrum antibiotic, with antibacterial, anti-thyroid, diuretic, anti-carbonic anhydrase, and antimalarial properties.[9,10]

Sulfonamide derivatives remain widely used as antimicrobial agents due to their affordability, low toxicity, and potent activity against bacterial infections. Following this pressing need, an increasing interest has emerged in SD–metal complexes. These complexes are formed *via* coordination of the sulfonamide moiety to metal ions, such as sodium,[11] calcium,[12] copper,[13] zinc,[14] nickel,[15] cobalt,[16] and manganese.[17] The complexes can be obtained by various synthetic methods such as reflux, solvothermal and microwave assisted synthesis.

Zinc–sulfadiazine (ZnSD) complexes have also shown efficacy in preventing bacterial infections in animal burns.[14]

AgSD is widely employed in topical antibiotic therapy, reducing the bacterial load and promoting wound healing. Structurally, it contains a silver cation tetra-coordinated to 3 N-atoms and one O-atom from three deprotonated SD molecules, and each SD interacts with three different Ag^+ ions. AgSD can release Ag^+ ions, which disrupt cell membranes and DNA replication, and SD that acts bacteriostatically by inhibiting folic acid synthesis through competitive binding with *para*-aminobenzoic acid. However, the polymeric nature of AgSD limits its aqueous solubility and consequently reduces its efficacy and formulation compatibility. Therefore, new strategies are desired to increase solubility while improving bioavailability and antibacterial efficacy.[18]

Traditionally, AgSD is synthesized *via* a six-step solution-based process,[19] the last one being the formation of the silver complex through the reaction of silver nitrate in water at 60 °C for 10 min. The resulting precipitate was washed with cold water and dried. Silver's long-recognized antimicrobial properties have led to its use in various forms, such as $AgNO_3$, silver zeolites, and silver nanoparticles (AgNPs), for treating burns and chronic wounds.[20]

Despite their widespread use, solution-based synthesis methods have certain limitations in terms of safety and environmental impact. These methods typically involve the use of organic solvents, which can be difficult to handle and pose risks such as flammability, toxicity, and environmental contamination. Solvents used in large quantities generate significant waste that must be disposed of properly. In addition, the use of high temperatures and pressures in solution-based methods can further contribute to safety hazards and energy consumption. In contrast, mechanochemistry offers an alternative synthetic approach that overcomes many of the limitations associated with solution-based methods.[21]

In mechanochemistry, chemical reactions are carried out using mechanical force, typically by grinding, milling or high-energy ball milling. This technique offers several advantages such as improved safety, reduced solvent usage and low waste generation, improved reaction kinetics and general versatility. Mechanochemistry is a green and environmentally friendly synthetic technique whose application has grown tremendously in the last two decades and has recently become one of the top ten IUPAC technologies foreseen to change the world.[22]

The millennia-old technique regained prominence in crystal engineering and polymorphism in the 1980s and is now re-emerging as a simple, clean, and straightforward synthetic method for organic, metal–organic, coordination, and supramolecular syntheses. It evolved from being simply a solvent-free alternative to a main synthetic technique leading to reduced reaction times, higher yields, product selectivity and completely unexpected reaction products that are impossible to attain in solution.[23] A mechanochemical reaction, defined as "a chemical reaction that is induced by the direct absorption of mechanical energy"[24] when grinding together two or more compounds, is also affected by the addition of solvents, ions, ionic liquids and other additives used to augment, direct or enable reactivity. The most commonly used mechanochemical techniques are: neat grinding (NG), where no solvent is added, liquid assisted grinding (LAG), in which catalytic amounts of solvents are used, ion and liquid-assisted grinding (ILAG), in which catalytic amounts of solvent and an ionic salt are added to the reaction, and lastly and most recently, polymer-assisted grinding (POLAG), that uses polymers to promote the reaction.[23,25,26]

In particular, AgSD is typically synthesized by the reaction of $AgNO_3$ with SD in an aqueous or organic solvent in a (1 : 1) ratio, under the conditions previously summarized. However, Sović *et al.*[3] reported the first mechanochemical preparation of AgSD, by milling silver nitrate $AgNO_3$ and sulfadiazine in a 1 : 1 ratio, under very specific conditions. Here, a new ball milling process is proposed, and a new AgSD coordination compound is presented.

Results and discussion

The mechanochemical preparation of AgSD, starting from $AgNO_3$ and SD has been reported to require very specific conditions, namely, the mandatory use of either 25 or 10% aqueous ammonia solution. This reaction was carried out in poly(methylmethacrylate) (PMMA) grinding jars, at a frequency of 30 Hz, and reaction times between 30 and 90 minutes.[3]

The main goal of this study was to investigate the possible optimization of the mechanochemical synthesis of silver–sulfadiazine complexes. A comprehensive screening

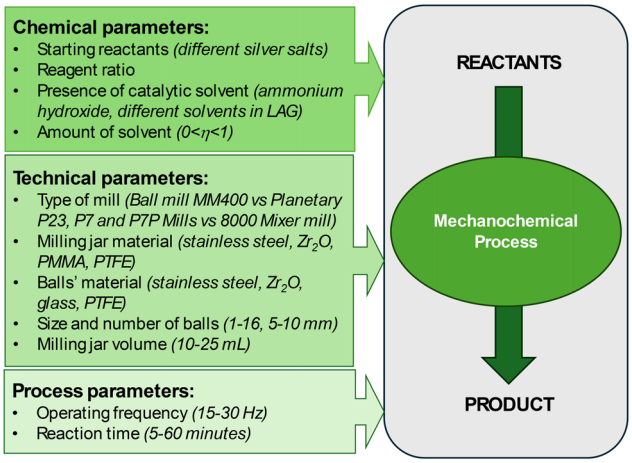

Chart 1 Schematic representation of selected parameters that may influence mechanochemical reactions. Image adapted from ref. 24 with the permission of Royal Society of Chemistry.

involving several variables (Chart 1), such as starting materials, presence of a catalytic solvent, amount of solvent (η), type of mill, grinding jar material, and balls' materials, led to the optimization of the synthesis conditions of a previously known form and the disclosure of a new complex.

The use of silver oxide and sulfadiazine as starting materials and using catalytic amounts ($\eta < 1$ μL mg^{-1}) of ethanol led to the formation by LAG of the previously reported AgSD[27] reported at the Cambridge Structural Database (CSD)[28] as the SULPMS form (Fig. 2). Even though the synthesis of this form had been reported both by solution and under mechanochemical conditions, a new procedure is disclosed herein, resulting from an optimization of the reaction conditions dismissing the addition of ammonium hydroxide to the reaction media, which presents an advantage.

The use of different silver salts as starting materials was another parameter tested in the synthesis of these Ag–sulfadiazine complexes. No reaction occurred when using silver chloride as starting material. On the other hand, silver sulfate did not lead to any reaction, prior to the addition of ammonium hydroxide, but with the addition of ammonium hydroxide, Ag_2SO_4 led to the formation of the known AgSD reported in the CSD[28] as the SULPMS form.[27]

On the other hand, $AgNO_3$ led to the formation of a new compound (**AgSD-NO_3**) by LAG. This new form was found to be highly reproducible using different mills (ball mills *vs.* planetary mills) and grinding jars' materials (ZrO_2, stainless steel, PMMA, glass, Teflon).

In order to explore the influence of different stress phenomena towards the selective formation of a specific crystalline form of silver sulfadiazine, the preparation of the **AgSD-NO_3** metallodrug was explored by modulating the amount of energy transferred to the powders by systematically investigating mechanochemical processing conditions combining both technical (*e.g.*, type of ball-mill, milling media, size and number of milling balls, milling jar volume) and process parameters (*e.g.*, operating frequency, continuous milling or by cycles). In addition to hard milling media such as zirconium oxide and stainless steel (SS), softer milling media were also explored. Indeed, the powders were also milled in PTFE or PMMA jars, each time in the presence of balls having different sizes, density and hardness (*e.g.*, glass, PFTE, zirconium oxide or stainless steel). All the reactions were conducted under liquid-assisted grinding (LAG) conditions, keeping the amount of water (LAG solvent) constant (η = 0.25 μL mg^{-1}) for all the experiments, and independently on the reaction scale (comprised between 0.456 mmol and 2.856 mmol). As a general trend, and for independency on the mechanochemical processing conditions used, the 'snowball' effect[29] was observed for all the samples. Even if the full recovery of the final product could not be achieved for rheological reasons (powder sticking to the balls and to the walls of the vessel), PXRD analyses could be carried out on all samples, even after ageing.

A comparison between the PXRD patterns of the starting materials (sulfadiazine and silver nitrate reacted in equimolar amount) and with the PXRD pattern of the commercial metallodrug silver sulfadiazine (SULPMS)[27] shows that not only the reaction was complete, but a new form was obtained, in all the mechanochemical conditions explored (*c.f.*, Tables S1–S4, SI). Moreover, compared to solution-based synthesis,[19] the mechanochemical preparation of silver sulfadiazine did not require any heating or post-

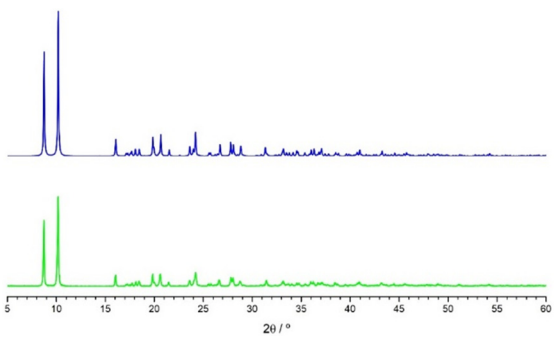

Fig. 2 PXRD diffractograms collected at λ (Cu Kα_1) = 1.54056 Å of AgSD reported as SULPMS (green) experimentally obtained by the LAG method and simulated (blue).

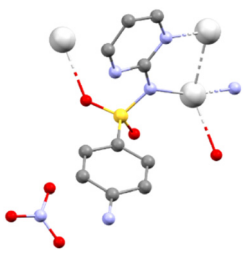

Fig. 3 Crystal structure of the new **AgSD-NO_3** (colour code: red – oxygen; blue – nitrogen; grey – carbon; yellow – sulfur; light grey – silver).

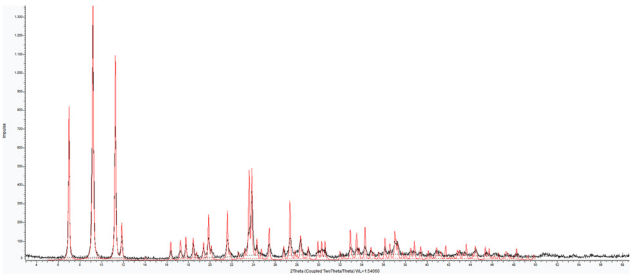

Fig. 4 PXRD of the new **AgSD-NO$_3$** (black) compared with the theoretical pattern (red).

reaction operation, the product being recovered pure directly from the jar.

Structural elucidation of AgSD-NO$_3$

The structure of the new form **AgSD-NO$_3$** (Fig. 3) was elucidated using high-resolution synchrotron PXRD data (Fig. 4). The resulting structure revealed the presence of a nitrate counterion in the crystal structure, in agreement with the elemental analysis carried out for this compound presented in the general description section.

It is rather interesting to compare the crystal structure of the newly reported **AgSD-NO$_3$** with the crystal structure of the previously known AgSD form.

2-Sulfanilamidopyrimidinesilver(I) (silver sulfadiazine, AgSD) crystallizes in the monoclinic space group $P2_1/c$. Each silver(I) center adopts a distorted trigonal bipyramidal geometry, coordinated by one silver(I) atom, three nitrogen atoms (two from the pyrimidine ring and one imido nitrogen) and one oxygen atom from the sulfonyl group. The equatorial plane consists of bonds to N1 (pyrimidine, 2.205(6) Å), N3 (imido, 2.277(6) Å), and O3 (sulfonyl, 2.571(6) Å), while the axial positions are occupied by N7 (pyrimidine, 2.459(6) Å) and a symmetry-related silver atom at 2.916(1) Å.

This coordination links silver atoms into double-stranded polymeric chains along the *a*-axis. Like the situation in SULPMS, in **AgSD-NO$_3$**, each silver atom is also coordinated in a highly distorted trigonal bipyramidal geometry, with a τ_5 parameter of 0.54 (if τ_5 is close to 0 the geometry is square pyramidal, while if τ_5 is close to 1 then the geometry is trigonal bipyramidal).[30] Here, the coordination environment is formed by two nitrogen atoms (imido, d_{Ag-N} = 2.0715 Å; pyrimidine d_{Ag-N} = 1.9914 Å) and two sulfonyl oxygen atoms from two sulfadiazine ligands (d_{Ag-O} = 2.5030 and 2.7236 Å). The coordination environment is completed by a symmetry related Ag atom at 2.8155(2) Å.

In AgSD, the structure features interconnected chains. These chains are further organized into planar sheets through hydrogen bonds between amine hydrogens and sulfonyl oxygens, extending the supramolecular network in the *b*- and *c*-direction. Overall, silver sulfadiazine's stability arises from its layered architecture combining coordination polymers and hydrogen-bonded sheets.[27]

In **AgSD-NO3**, the coordination leads to formation of chains along the *b*-axis. In the *a*–*c* plane these chains are arranged in a hexagonal close packing separated by the NO_3^- ions (Fig. 5).

Antimicrobial activity

Even though silver sulfadiazine is water-insoluble, it dissolves slowly in biological fluids.[31] Therefore it was possible to proceed with testing the antimicrobial activity of the two silver sulfadiazine compounds. Their median minimum inhibitory concentration (MIC) values were calculated using the microdilution method[32,33] and compared with the activity of the starting materials. Strains were selected so that Gram-positive (*Staphylococcus aureus MRSA* and *Mycobacterium smegmatis*) and Gram-negative (*Escherichia coli* and *Pseudomonas aeruginosa*) bacteria were represented, as well as yeasts (*Candida albicans* and *Saccharomyces cerevisiae*). Gram-positive *S. aureus* MRSA was included to broaden the essays to include multi-resistant strains.

The results obtained (Table 1) show that the silver–sulfadiazine compounds (SULPMS and AgSD-NO$_3$) present increased antimicrobial activity against *S. aureus* MRSA, *P. aeruginosa* and *E. coli* relative to sulfadiazine alone.

In fact, their effect on *S. aureus* MRSA is very striking as this strain is the least sensitive to sulfadiazine, among the microorganisms tested here. Comparing both Ag–sulfadiazine forms, their activity against the tested strains is similar, suggesting that both compounds effectively deliver bioavailable Ag^+. Differences in solubility or release kinetics might influence their performance synergistically in specific environments.

It can be noticed that silver oxide is a better antimicrobial agent than silver nitrate, except for *M. smegmatis*. For *M.*

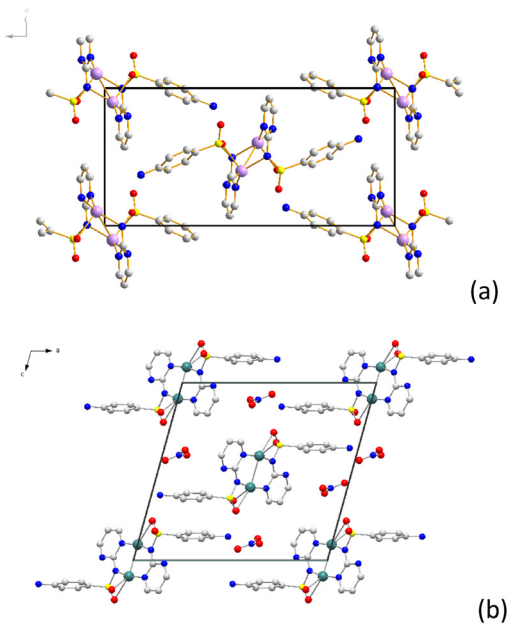

Fig. 5 Supramolecular packing of **AgSD-NO$_3$** depicting the formation of (a) chains along the *b*-axis and (b) the hexagonal array in the *a*–*c* plane.

Table 1 Determination of the MIC values (μg mL^{-1}) of the synthesized Ag–sulfadiazine compounds and the starting materials for *Candida albicans* and *Saccharomyces cerevisiae* (yeasts), *Escherichia coli* and *Pseudomonas aeruginosa* (Gram-negative bacteria) and *Staphylococcus aureus* MRSA and *Mycobacterium smegmatis* (Gram-positive bacteria) after 24 h for bacteria and 48 h for yeasts

	Microorganisms					
	Gram-positive bacteria		Gram-negative bacteria		Yeasts	
Compounds	*M. smegmatis*	*S. aureus MRSA*	*P. aeruginosa*	*E. coli*	*C. albicans*	*S. cerevisiae*
AgSD (refcode SULPMS)	15.625	31.25	15.625	15.625	62.5	62.5
AgSD-NO_3	15.625	31.25	15.625	15.625	62.5	62.5
$AgNO_3$	15.625	15.625	15.625	15.625	31.25	31.25
Ag_2O	19.625	9.813	9.813	9.813	9.813	9.813
Sulfadiazine	15.625	125	62.5	31.25	62.5	62.5
Negative control	125	125	62.5	125	125	62.5
Positive control	<0.488 (Van)	<0.488 (Van)	<0.488 (Nor)	<0.488 (Nor)	7.81 (Nys)	15.63 (Nys)

Legend: positive controls: Nys – nystatin; Nor – norfloxacin; Van – vancomycin. Negative control: DMSO.

smegmatis, the presence of the silver frameworks, sulfadiazine or the silver salts provoked a similar reaction as their MIC values are very similar.

The effect of the reported form of AgSD and **AgSD-NO_3** (and silver nitrate) on *P. aeruginosa* and *E. coli* demonstrates higher impact compared to sulfadiazine alone, due to the synergistic effect of silver. Although, *E. coli* is more sensitive to sulfadiazine than *P. aeruginosa*.

For the tested yeasts (*S. cerevisiae* and *C. albicans*) even though silver nitrate has an important impact in the growth of these organisms, the compounds containing sulfadiazine display a similar MIC. This means the presence of the silver atom is not interfering with the cell viability of these strains.

Interestingly, there was the opportunity to test a multi-resistant *S. aureus* strain, and the results show that although sulfadiazine has no great effect on the viability of this strain, the compounds containing silver atoms highly decrease their MIC values.

The results show that the new silver sulfadiazine compounds displayed increased antimicrobial activity when compared to sulfadiazine itself. This effect can be associated with the synergy between sulfadiazine and silver metal centres, the latter being well-known for their antimicrobial efficiency.[34–36] Moreover, these striking and very promising findings provide a valuable strategy to reuse the available antibiotics and obtain new and powerful ACFs to battle bacteria like *P. aeruginosa*, *E. coli* and *S. aureus*, which are responsible for several nosocomial infections and highly capable of developing resistance mechanisms to the existing antibiotics.[37,38]

Experimental

Reagents

The reagents and solvents were purchased from commercial sources and used without further purification.

Synthesis of the compounds

Synthesis of AgSD (CCDC ref code SULPMS). LAG using a Retsch MM400 ball mill: AgSD was obtained by grinding sulfadiazine (0.5462 mmol) and silver oxide (0.2731 mmol) in a proportion of 2 : 1 with the addition of 50 μL distilled water (η = 0.25 μL mg^{-1}), with two 7 mm stainless steel balls for 30 minutes in a MM400 ball mill at 30 rpm.

Synthesis of AgSD-NO_3

Manual grinding. Compound **AgSD-NO_3** was obtained by manually grinding sulfadiazine (0.2380 mmol) and silver nitrate (0.2380 mmol) using an agate mortar and pestle in a proportion of 1 : 1 for 25 minutes with the addition of 140 μL distilled water (η = 1.40 μL mg^{-1}).

LAG optimization of operating conditions using a Retsch MM400 ball mill. Compound **AgSD-NO_3** was obtained by grinding sulfadiazine (0.4760 mmol) and silver nitrate (0.4760 mmol), in the presence of 50 μL distilled water (η = 0.25 μL mg^{-1}) for 30 minutes, with two 7 mm stainless steel balls in a 10 mL snap closure stainless steel jar using a MM400 ball mill at 30 rpm.

The mechanochemical preparation of **AgSD-NO_3** was performed under several other reaction conditions (amounts of starting materials, solvent, total balls weight and reaction time), using different milling media (SS, ZrO_2, Agate, PMMA and PTFE) and milling apparatus (vibrating ball-mills both horizontally or vertically, shaker mill, and planetary ball-mill). All the reactions were conducted under liquid-assisted grinding (LAG) conditions, keeping the amount of water (LAG solvent) constant (η = 0.25 μL mg^{-1}) for all the experiments, and independently on the reaction scale (comprised between 0.456 mmol and 2.856 mmol). All the detailed mechanochemical conditions are reported in Tables S1–S4 (SI).

Many different recrystallizations of the obtained powder were performed in different solvents: H_2O, ethanol, methanol, ethyl acetate, acetone, and acetonitrile. However, no single crystal was grown, and structure elucidation was carried out from high-resolution synchrotron data.

General characterization

Powder X-Ray Diffraction (PXRD) data were collected in a D8 Advance Bruker AXS θ–θ diffractometer, equipped with a LYNXEYE-XE detector, copper radiation source (Cu Kα, λ =

Table 2 Elemental analysis of the new sulfadiazine–silver form ($C_{10}H_{10}AgN_5O_5S$)

	Elemental analysis (%)				
	1	2	Average	Expected	Δ
N	16.35	16.27	16.310	16.67	0.360
C	28.27	28.30	28.285	28.59	0.305
H	2.11	2.01	2.06	2.40	0.34
S	8.14	8.03	8.085	7.63	−0.455

1.5406 Å), operated at 40 kV and 30 mA, and with the following data collection parameters: 3–60° 2θ range, step size of 0.02° and 0.6 s per step and 3–37° 2θ range, step size of 0.02° and 0.5 s per step. The diffractograms were used to ascertain bulk material purity of the synthesized compounds, by comparing the calculated (from SCXRD data) and experimental PXRD patterns. MERCURY 2024.2.0 (ref. 39) was used to obtain calculated patterns from single-crystal data.

Structural analysis of AgSD-NO_3. PXRD measurements were conducted on a Bruker D8 Discover diffractometer (Cu Kα1 radiation, λ = 1.5406 Å), which was equipped with a Johansson monochromator and a LYNXEYE detector. Samples of **AgSD-NO_3** in 0.5 mm glass capillaries were scanned at a spin rate of 60 min^{-1} from 5–60° 2θ with a step size of 0.009° and an acquisition time of 2 s per step. The structure solution utilised EXPO2014 (ref. 40) and TOPAS.[41] Initial models were generated using simulated annealing in DASH, with molecular fragments sourced from the Cambridge Structural Database (CSD entry: SULPMS). Full molecular flexibility was permitted during annealing. Rietveld refinements in TOPAS optimised the scale factors, background, atomic positions and isotropic displacement parameters across the full 2θ range. Final Rietveld refinement against experimental data confirmed the AgSD-NO_3 structure.

Elemental analysis. Elemental analyses for carbon (C), hydrogen (H), nitrogen (N) and sulfur (S) (Table 2) were performed in a Fisons CHNS/O analyser Carlo Erba Instruments EA-1108 equipment, at the IST Analyses Laboratory.

Antimicrobial activity assays. The synthesized compounds and respective starting materials were tested against yeasts (*Candida albicans* ATCC 10231, *Saccharomyces cerevisiae* ATCC 2601), Gram-negative (*Escherichia coli* ATCC 25922, *Pseudomonas aeruginosa* ATCC 27853) and Gram-positive bacteria (*Staphylococcus aureus* MRSA CIP 106760, *Mycobacterium smegmatis* ATCC 607) for the determination of their MIC values. These values were determined by the microdilution method.[30,31,40,42] Briefly, 100 μL of Mueller–Hinton (for bacteria) or Sabouraud Dextrose (for yeasts) liquid culture medium were added to all the 96-wells of the microtiter plates. Then, 100 μL of the testing compounds at a concentration of 1 mg mL^{-1} in DMSO were added to the first well. Serial dilutions of (1 : 2) were performed and 10 μL of microbial inoculum was added to each well. The microtiter plates were incubated at 37 °C for 24 h and 48 h (for bacteria and yeasts, respectively), and their growth was visually assessed.

Conclusions

The obtained results highlight the importance of mechanochemistry as a green, sustainable, and fast solid state synthetic technique to be considered and applied in the production of novel metal frameworks.

The enhanced antimicrobial potential of the silver sulfadiazine frameworks compared to sulfadiazine alone is clear in this work. The observed synergy between sulfadiazine and silver centres, well-recognized for their antimicrobial properties, offers a plausible explanation for this improvement. Importantly, this can be a promising approach towards repurposing of existing antibiotics and the development of powerful antimicrobial compounds, with mechanochemistry playing a fundamental role in this scope. Such advances could play a critical role in combating drug-resistant bacteria like *P. aeruginosa*, *E. coli*, and *S. aureus*, which are major culprits of nosocomial infections and pose significant challenges to modern medicine.

Author contributions

D. R. F.: mechanochemical synthesis and data curation; A. P.: mechanochemical synthesis and data curation; P. C. A.: methodology for biological essays, data curation, and manuscript editing; P. R.: methodology for the biological essays and manuscript editing; C. S. B. G.: data curation and manuscript editing; M. T. D.: data curation; I. H.: data curation and manuscript editing; E. C.: conceptualisation, data curation, manuscript editing, and funding; F. E.: conceptualisation, data curation, manuscript editing, and funding; V. A.: design, conceptualisation, data curation, funding, initial draft preparation, and manuscript editing. The manuscript was written through the contributions of all authors. All authors approved the final version of the manuscript. All authors contributed equally.

Conflicts of interest

There are no conflicts to declare.

Data availability

The data supporting this article have been included as part of the SI.

Supplementary Information available: SI contains the experimental protocols for the mechanochemical synthesis of AgSD-NO_3 under different processing conditions, by vibrating, shaker mill and planetary ball-mills, at different scales. Structural and stability data are also included. See DOI: **https://doi.org/10.1039/D5CE00572H**.

Crystallographic data of compound AgSD-NO_3 has been deposited at the Cambridge Crystallographic Data Centre

under CCDC 2455885, and can be accessed upon request Search – Access Structures.

Acknowledgements

V. A., D. R. F., P. C. A., M. T. D., C. S. B. G. and P. R. acknowledge funding from Fundação para a Ciência e a Tecnologia (FCT, Portugal) for the CQE projects UIDB/00100/2020 (**https://doi.org/10.54499/UIDB/00100/2020**), and UIDP/00100/2020 (**https://doi.org/10.54499/UIDP/00100/2020**); IMS project LA/P/0056/2020 (**https://doi.org/10.54499/LA/P/0056/2020**); CBIOS projectsUIDP/04567/2020 (**https://doi.org/10.54499/UIDP/04567/2020**) and UIDB/04567/2020 (**https://doi.org/10.54499/UIDB/04567/2020**); and LAQV projects UID/50006/2023 and LA/P/0008/2020 (**https://doi.org/10.54499/LA/P/0008/2020**). A. P. and E. C. acknowledge Région Occitanie (France) for the Pre-Maturation 2020 – MECHAPI grant (ESRPREMAT – 00262). This article is based upon work from COST Action CA18112 'Mechanochemistry for Sustainable Industry',[43–46] supported by COST (European Cooperation in Science and Technology).[47] COST (European Cooperation in Science and Technology) is a funding agency for research and innovation networks, helping to connect research initiatives across Europe and enable scientists to grow their ideas by sharing them with their peers. This boosts their research, career and innovation. **https://www.cost.eu**. E. C. is grateful to Julien Fullenwarth (Institut Charles Gerhardt de Montpellier, ICGM, France), for the access to SPEX shaker-mill 8000.

References

1 World Health Organization, Burns, **https://www.who.int/news-room/fact-sheets/detail/burns**, (accessed 22 April 2025).
2 V. Andre, A. Hardeman, I. Halasz, R. S. Stein, G. J. Jackson, D. G. Reid, M. J. Duer, C. Curfs, M. Teresa Duarte and T. Friscic, *Angew. Chem., Int. Ed.*, 2011, **50**, 7858–7861.
3 I. Sović, S. Lukin, E. Meštrović, I. Halasz, A. Porcheddu, F. Delogu, P. C. Ricci, F. Caron, T. Perilli, A. Dogan and E. Colacino, *ACS Omega*, 2020, **5**, 28663–28672.
4 World Health Organization, WHO Model List of Essential Medicines – 23rd List, 2023, **https://www.who.int/publications-detail-redirect/WHO-MHP-HPS-EML-2023.2002**, (accessed 02 June 2025).
5 H. Stöber and W. DeWitte, *Anal. Profiles Drug Subst.*, 1982, **11**, 523–551.
6 R. S. Vardanyan and V. J. Hruby, *Synthesis of Essential Drugs*, Elsevier, Amsterdam, 2006, pp. 499–523.
7 S. Chernousova and M. Epple, *Angew. Chem., Int. Ed.*, 2013, **52**, 1636–1653.
8 S. Chernousova and M. Epple, Silver as Antibacterial Agent: Ion, Nanoparticle, and Metal, *Angew. Chem., Int. Ed.*, 2013, **52**, 1636–1653.
9 T. D. M. Pham, Z. M. Ziora and M. A. T. Blaskovich, *MedChemComm*, 2019, **10**, 1719–1739.
10 M. I. Andersson and A. P. MacGowan, *J. Antimicrob. Chemother.*, 2003, **51**, 1–11.
11 G. Campbell, R. Fisher, A. R. Kennedy, N. L. C. King and R. Spiteri, *Acta Crystallogr., Sect. C:Struct. Chem.*, 2018, **74**, 472.
12 J. Sun, C. Xie, X. Zhang, Y. Bao, B. Hou, Z. Wang, J. Gong, H. Hao, Y. Wang, J. Wang and Q. Yin, *Org. Process Res. Dev.*, 2016, **20**, 780.
13 C. J. Brown, D. S. Cook and L. Sengier, *Acta Crystallogr., Sect. C: Cryst. Struct. Commun.*, 1987, **43**, 2332.
14 F. Pan, R. Wang and U. Englert, *Inorg. Chem.*, 2012, **51**, 769.
15 W.-B. Shi, A.-L. Cui and H.-Z. Kou, *Polyhedron*, 2015, **99**, 252.
16 M. Rocha, O. E. Piro, G. A. Echeverría, A. C. Pastoriza, M. A. Sgariglia, J. R. Soberón and D. M. Gil, *J. Mol. Struct.*, 2019, **1176**, 605.
17 T.-J. He, Y.-S. Tan, Y.-Q. Gu, Z.-F. Chen and H. Liang, *Acta Crystallogr., Sect. E: Struct. Rep. Online*, 2010, **66**, m684.
18 X. Liu, H. Gan, C. Hu, W. Sun, X. Zhu, Z. Meng, R. Gu and Z. Wu, *Int. J. Nanomed.*, 2018, **14**, 289–300.
19 A. D. L. Borges, G. Del Ponte, A. F. Neto and I. Carvalho, *Quim. Nova*, 2005, **28**, 727–731.
20 Wounds International, Best Practice Guidelines: Effective Skin and Wound Management in Non-Complex Burns, **https://woundsinternational.com/wp-content/uploads/2023/02/e472ecca6a9316d2648ea567a710e97a.pdf**, (accessed 22 April 2025).
21 T. Friščić, C. Mottillo and H. M. Titi, *Angew. Chem.*, 2020, **132**, 1030–1041.
22 F. Gomollón-Bel, *Chem. Int.*, 2019, **41**, 12–17.
23 J.-L. Do and T. Friščić, *ACS Cent. Sci.*, 2017, **3**, 13–19.
24 The IUPAC compendium of chemical terminology, *The Gold Book*, ed. V. Gold and A. McNaught, International Union of Pure and Applied Chemistry (IUPAC), 2025, **https://goldbook.iupac.org/**, (accessed, 31 May 2025).
25 S. L. James, C. J. Adams, C. Bolm, D. Braga, P. Collier, T. Friščić, F. Grepioni, K. D. M. Harris, G. Hyett, W. Jones, A. Krebs, J. Mack, L. Maini, A. G. Orpen, I. P. Parkin, W. C. Shearouse, J. W. Steed and D. C. Waddell, *Chem. Soc. Rev.*, 2012, **41**, 413–447.
26 A. Mascitti, M. Lupacchini, R. Guerra, I. Taidakov, L. Tonucci, N. d'Alessandro, F. Lamaty, J. Martinez and E. Colacino, *Beilstein J. Org. Chem.*, 2017, **13**, 19–25.
27 N. C. Baenziger and A. W. Struss, *Inorg. Chem.*, 1976, **15**, 1807.
28 C. R. Groom, I. J. Bruno, M. P. Lightfoot and S. C. Ward, *Acta Crystallogr., Sect. B: Struct. Sci., Cryst. Eng. Mater.*, 2016, **72**, 171–179.
29 M. Carta, S. L. James and F. Delogu, *Molecules*, 2019, **24**, 3600.
30 A. W. Addison, N. T. Rao, J. Reedijk, J. van Rijn and G. C. Verschoor, *J. Chem. Soc., Dalton Trans.*, 1984, 1349–1356.
31 C. L. Fox Jr., *Arch. Surg.*, 1968, **96**, 184–188.
32 F. Siopa, T. Figueiredo, R. F. M. Frade, I. Neto, A. Meirinhos, C. P. Reis, R. G. Sobral, C. A. M. Afonso and P. Rijo, *ChemistrySelect*, 2016, **1**, 5909–5916.
33 J. H. Jorgensen, Clinical and Laboratory Standards Institute, *Methods for Dilution Antimicrobial Susceptibility Tests for Bacteria That Grow Aerobically*, CLSI standard M07, Wayne, PA, 12th edn, 2022.

34 J. W. Alexander, *Surg. Infect.*, 2009, **10**, 289–292.
35 L. Poirel, J.-Y. Madec, A. Lupo, A.-K. Schink, N. Kieffer, P. Nordmann, S. Schwarz, M. Aarestrup Frank, J. Shen and L. Cavaco, *Microbiol. Spectrum*, 2018, **6**, ARBA-0026-2017.
36 A. D. Politano, K. T. Campbell, L. H. Rosenberger and R. G. Sawyer, *Surg. Infect.*, 2013, **14**, 8–20.
37 T. J. Foster, *FEMS Microbiol. Rev.*, 2017, **41**, 430–449.
38 Z. Pang, R. Raudonis, B. R. Glick, T.-J. Lin and Z. Cheng, *Biotechnol. Adv.*, 2019, **37**, 177–192.
39 C. F. Macrae, I. Sovago, S. J. Cottrell, P. T. A. Galek, P. McCabe, E. Pidcock, M. Platings, G. P. Shields, J. S. Stevens, M. Towler and P. A. Wood, *J. Appl. Crystallogr.*, 2020, **53**, 226–235.
40 A. Altomare, F. Ciriaco, C. Cuocci, A. Falcicchio and F. Fanelli, *Powder Diffr.*, 2017, **32**(S1), S123–S128.
41 A. A. Coelho, *J. Appl. Crystallogr.*, 2018, **51**, 210–218.
42 P. C. Alves, P. Rijo, C. Bravo, A. M. M. Antunes and V. André, *Molecules*, 2020, **25**, 2374.
43 COST Action CA18112, Mechanochemistry for Sustainable Industry (MechSustInd), **https://www.mechsustind.eu/**, (accessed 02 June 2025).
44 J. G. Hernández, I. Halasz, D. E. Crawford, M. Krupicka, M. Baláž, V. André, L. Vella-Zarb, A. Niidu, F. García, L. Maini and E. Colacino, *Eur. J. Org. Chem.*, 2020, **2020**, 8–9.
45 J. Biela, M. Stalla, L. Rabe, D. Machado, G. Evers and S. Ansems, Impact Assessment Study on Innovation in COST Actions, November 2024, **https://www.cost.eu/uploads/2025/01/COST-Impact-Assessment-Innovation-112024.pdf**, (accessed 15 May 2025).
46 J. J. Saenz de La Torre, L. Flamarique, F. Gomollon-Bel and E. Colacino, *Open Res. Eur.*, 2025, **5**, 73.
47 COST – European Cooperation in Science and Technology, **https://www.cost.eu/**, (accessed 02 June 2025).

